Picosecond resolution measurements of NO_3 unimolecular decomposition. The $NO+O_2$ channel ☆

H.F. Davis, P.I. Ionov, S.I. Ionov and C. Wittig

Department of Chemistry, University of Southern California, Los Angeles, CA 90089-0482, USA

The title reaction has been studied with picosecond resolution at energies near threshold. Expansion cooled nitrate radicals were photoexcited to admixtures of $^2E'$ and ground state $^2A_2'$ levels, ensuring a unimolecular decomposition mechanism. NO was monitored by LIF. The dissociation rate is $\approx 1 \times 10^9$ s^{-1} just above the 16800 cm^{-1} $NO+O_2$ barrier and increases rapidly with energy, reaching 5.5×10^9 s^{-1} at 17040 cm^{-1}. A marked signal decrease at higher energies is attributed to NO_2+O dominating above its thermodynamic threshold. These observations support three-center $NO+O_2$ formation via $^2A_2'$.

1. Introduction

For a number of species, the mixing of zeroth-order ground and excited electronic states [1–7] enables visible and/or ultraviolet radiation to be used to prepare highly vibrationally excited levels of mainly ground electronic state character at well-defined energies above the threshold(s) for unimolecular reaction. Consequently, comparisons between measured decomposition rates and various theoretical models have provided insight into the transition state region [3,4,8–10]. For example, time-resolved, subpicosecond resolution measurements of NO production from NO_2 photolysis near reaction threshold have shown a structured increase in reaction rate with increasing energy [3,4], as predicted theoretically [11].

Though bond fission yielding two radical fragments is perhaps the most common class of unimolecular reaction, another important class involves the concerted breaking and forming of several chemical bonds. Well documented examples include: the elimination of H_2 from hydrocarbons [12]; the decomposition of formaldehyde to H_2+CO [5–7]; and three- and four-center eliminations of hydrogen halides from halogenated hydrocarbons [13–15]. In most cases, such concerted reactions are unfavorable dynamically due to a large barrier on the potential energy surface. In cases where the barrier is lower than the endothermicity for simple bond fission, concerted reactions may be possible, though their rates are expected to be smaller than for the corresponding bond fission reactions, due to relatively tight transition states. Clearly, direct determinations of reaction rates can provide insight into the saddle point regions of three-center concerted reactions.

The nitrate free radical and nitrates are of great importance in areas ranging from atmospheric chemistry [16,17] to energetic materials [18]. The two competing channels involved in the photochemistry of NO_3 are shown in fig. 1. Simple $O–NO_2$ bond rupture is the dominant photochemical process above its thermodynamic threshold of 17040 ± 90 cm^{-1} [19]. However, the potential energy barrier for the $NO+O_2$ channel lies slightly below $D_0(O–NO_2)$, and the NO quantum yield under collision-free conditions was shown to be 0.7 ± 0.1 near 588 nm (≈ 17000 cm^{-1}) [19]. At excitation energies below the $NO+O_2$ barrier, the fluorescence quantum yield is presumably unity [19–22]. The wavelength dependence for the two chemically distinct channels is complicated by NO_3 hot-band activity, leading to
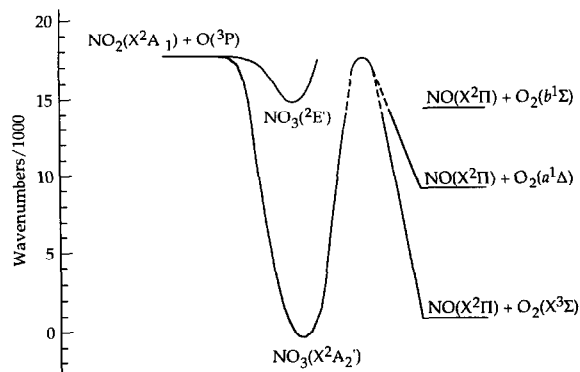
Fig. 1. Energy level diagram for NO_3 photodissociation. Thermodynamic quantities were obtained from ref. [19].

formation of both $NO_2 + O$ and $NO + O_2$ at excitation energies lower than the nominal 0 K thresholds stated above [19,23-25].

The absorption of a single photon having energy just below $D_0(O-NO_2)$ prepares NO_3 vibronic levels that are best described as admixtures of the electronically excited $^2E'$ state and the vibrationally excited $^2A_2'$ ground electronic state, i.e. the Douglas effect [19,22,26,27]. Unimolecular decomposition via a concerted three-center mechanism leads to $NO + O_2$, with O_2 believed to be formed primarily in the a $^1\Delta$ state [19]. Though it was not possible to obtain reaction rates directly in the previous study, isotropic center-of-mass product angular distributions suggested that parent lifetimes exceeded a rotational period of several picoseconds [19].

The physics and chemistry of molecular species having energies just below the lowest bond fission channel can be fascinating. In such cases, the "fission fragments" can reorient relative to each other in an orbiting (but weakly bound) collision complex. This facilitates the opening of other channels, as would occur for example in low-energy gas phase collisions. Since simple bond fission is energetically closed, channels involving complex bond rearrangements can have high quantum yields, independent of phase space bottlenecks, e.g. unity when only one channel is open. The present system is but one example.

In this Letter, time-resolved, picosecond resolution measurements of NO_3 unimolecular decomposition are reported. Rates were obtained by moni-

toring laser-induced fluorescence (LIF) of the $NO(X^2\Pi)$ product as the pump-probe delay was varied. The rates thus obtained are compared to estimates made by using RRKM theory.

2. Experimental

The configuration of the laser system used in the present experiments is essentially the same as that described previously [3,4,28]. A Coherent 702-1 dye laser operating on rhodamine 6G was pumped by a 76 MHz mode-locked Nd:YAG laser (Spectron SL903). The dye laser output was amplified at 10 Hz by a three-stage dye amplifier pumped by 532 nm pulses (70 ps, 30 mJ) from a regenerative amplifier (Continuum RGA 69-10). Approximately 80% of the tunable output near 590 nm (≈ 1 ps, ≤ 1 mJ, 60 cm^{-1} bandwidth) was used for NO_3 excitation. The remainder was focused into a cell containing D_2O for supercontinuum generation. A grating monochromator selected 452 nm radiation, which was amplified to ≈ 150 μJ in a two-stage dye amplifier pumped at 355 nm (60 ps, 30 mJ) using the RGA. A BBO crystal doubled this radiation to 226 nm (1 ps, ≈ 30 μJ) for LIF detection of NO via the (0, 0) band of the A $^2\Sigma \leftarrow X^2\Pi$ system.

Variable pump-probe delays were introduced by retroreflection of the pump pulse through a computer controlled translation stage. The need for delays > 1 ns necessitated long travel. To minimize beam walk-off due to imperfections in the translation stage, after the initial pass the pump pulse was retroreflected from a fixed periscope for a second pass through the delay stage. This doubled the pump-probe delay and partially compensated for beam walk-off. The pump and probe pulses were combined on a dichroic mirror and were focused to ≈ 2 mm diameter at the interaction region.

NO_3 was generated by N_2O_5 pyrolysis [19]. A mixture of 5% N_2O_5 in He (≈ 50 Torr) was expanded continuously into the vacuum chamber with the nozzle aperture resistively heated to $\approx 300°C$. The amount of NO_3 was optimized by adjusting the nozzle temperature while monitoring NO_3 via $^2E' \leftarrow ^2A_2'$ LIF near 662 nm [20,21] using a nanosecond Nd:YAG pumped dye laser. In the picosecond photodissociation experiments, the intensity of

the NO LIF signal showed the same dependence on nozzle temperature as did the NO_3 LIF intensity, i.e. decreasing at temperatures higher than 300°C due to thermal decomposition of NO_3. This is good evidence that the picosecond photodissociation signals derive from NO_3 photolysis. Specifically, if the NO had derived from two-photon NO_2 excitation, rather than from NO_3 photodissociation, the NO LIF intensity should have continued to increase at nozzle temperatures above 300°C, since the NO_2 concentration increases with temperature [29,30]. Further evidence that the NO signals result from NO_3 photoexcitation is that the wavelength dependence closely matches that observed recently in experiments in which both momentum matched fragments (NO and O_2) were detected following NO_3 photodissociation [19]. Since N_2O_5 does not absorb visible light [31] and has a negligible concentration at 300°C [30], its photolysis cannot contribute to the NO product observed in this experiment.

The laser system was operated under conditions similar to those reported recently in which pump–probe cross correlations were determined by difference frequency generation in a BBO crystal [3,4,28]. In those experiments, the cross correlations were measured to be 0.5–1.0 ps, more than two orders of magnitude shorter than the fastest experimental risetime observed in the present experiments. Thus, data were fitted assuming delta function pulses.

3. Results and discussion

The appearance of NO(X $^2\Pi$) from single photon excitation of NO_3 near 590 nm is attributed to the reactions

$$NO_3 \rightarrow NO(X\,^2\Pi) + O_2(X\,^3\Sigma) , \qquad (1a)$$

$$NO_3 \rightarrow NO(X\,^2\Pi) + O_2(a\,^1\Delta) . \qquad (1b)$$
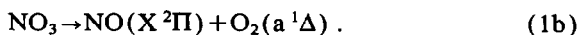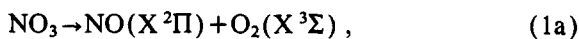
NO buildup times were obtained at nine excitation wavelengths and typical results are shown in fig. 2. The solid lines are fits to the data assuming single exponential behavior. As shown in fig. 3a, the smallest decomposition rate was observed near 16830 cm^{-1}. Rates were found to increase at higher photon energies, reaching 5×10^9 s^{-1} at 17040 cm^{-1}. As in previous studies of NO_3 photodissociation
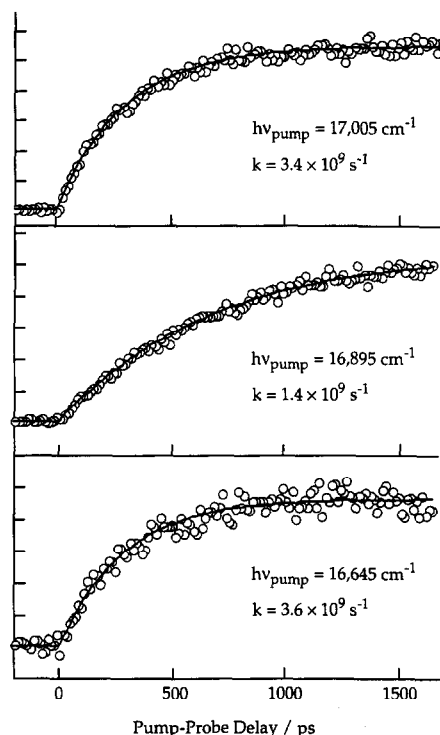

Fig. 2. NO LIF signal versus pump–probe delay for indicated excitation energies. The experimental points are fitted assuming single exponential decay.

[19,23,24], the NO signal intensity decreased sharply near 17040 cm^{-1}, becoming negligible above 17100 cm^{-1}. When tuning the pump laser to photon energies below 16835 cm^{-1}, the NO signal level also became very weak, and (surprisingly) the rates *increased* with decreasing photon energy. As discussed below, the signal observed at excitation energies below 16835 cm^{-1} is attributed to hot-band activity. The LIF signals became immeasurably small at photon energies below 16530 cm^{-1}. Figs. 3b and 3c show, respectively, the absorption cross section measured by Sander [32] for a 230 K sample and the NO signal intensity versus wavelength measured by Davis et al. using molecular beam photofragment translational energy spectroscopy [19].

A striking feature of the $NO+O_2$ channel is the narrow wavelength range over which it is observed. As in previous studies, the largest NO signals were seen near 16970 cm^{-1}, which corresponds to a peak in the NO_3 absorption spectrum. The barrier height
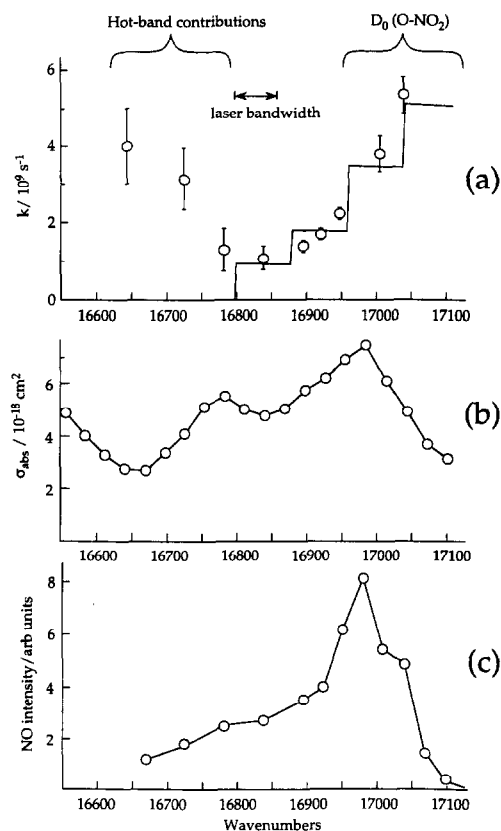
Fig. 3. (a) NO_3 unimolecular decay rate versus energy. Open circles are data and the solid line is from RRKM calculations. (b) NO_3 absorption cross section for a 230 K sample, from ref. [32]. (c) NO yield, from ref. [19].

for reaction (1) was recently determined from photofragment translational energy spectroscopy to be 16550 ± 280 cm^{-1} [19]. Previously, Nelson et al. [20,22] and Ishiwate et al. [21] had reported that at wavelengths longer than 595 nm the NO_3 LIF spectrum resembled the absorption spectrum. However, the LIF signal intensity decreased to zero below 595 nm, implying the onset of dissociation. The collision free fluorescence lifetime measured by Nelson and co-workers was 340 ± 20 μs [22], i.e. five orders of magnitude longer than the longest NO risetimes observed in our experiment. Thus, the cutoff of NO_3 fluorescence at 595 nm (16800 cm^{-1}) is a spectroscopic measure of the height of the potential energy barrier for the NO+O_2 channel. Since both studies reported that LIF signals fell to zero at 16800 cm^{-1}, and because vibrationally excited NO_3 molecules ab-

sorbing at wave-lengths near the nominal 0 K threshold will dissociate, the potential energy barrier for formation of NO+O_2 must lie close to 16800 cm^{-1}.

As in previous experiments [19,23,24], a sharp decrease in the NO signal intensity was seen above 17040 cm^{-1}. In a recent study of NO_3 photodissociation using photofragment translational energy spectroscopy [19], the sharp decrease in the NO and O_2 signals near 17040 cm^{-1} was attributed to opening of the NO_2+O channel

$$NO_3 \rightarrow NO_2(X\,^2A_1) + O(^3P) .\tag{2}$$
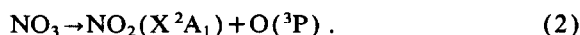
The rise in NO_2 yield was presumed due to surpassing its threshold for formation from internally cold NO_3, i.e. $D_0(O-NO_2) = 17040 \pm 90$ cm^{-1}.

RRKM rates were calculated by using a standard program [*1] [33]. Though NO_3 vibrational frequencies are well established [26], the transition state frequencies for formation of NO+O_2 are quite uncertain. Siegbahn [34] calculated the C_{2v} constrained barrier height for reaction and obtained a value of 67000 cm^{-1}, far higher than the experimental value. Boehm and Lohr [35,36] have performed generalized valence bond calculations on the $NO(X\,^2\Pi) + O_2(X\,^3\Sigma) \rightarrow NO_3$ potential energy surface in the region of the transition state. Their calculations suggested a tight transition state, and the saddle point energy was found to be very sensitive to departure from C_{2v} symmetry. It appears that effects due to symmetry breaking [34–38] and interactions between several electronic surfaces make theoretical estimates of NO_3 transition state parameters difficult.

RRKM calculations were performed by using $NO_3(X\,^2A_2')$ molecular frequencies of 363(2), 768, 1050 and 1768(2) cm^{-1} and the spectroscopically determined barrier height of 16800 cm^{-1}. Since the NO+O_2 channel participates only within 400 cm^{-1} of its potential energy barrier, the lowest transition state frequencies will contribute most to the reaction rate. The transition state vibrational frequencies (i.e. the lowest two) were used as adjustable parameters in the calculations. We focused on the energy range

---

[*1] An RRKM program written by W. Hase and D.L. Bunker was used in the calculations. The Whitten–Rabinovich approximation was used to calculate $p(E)$, while a direct count was used to calculate $N^*(E-E_0)$. Levels were sorted according to the symmetries allowed by optical selection rules. The foundations of the RRKM program are explained in ref. [33].

above 16800 cm^{-1}, i.e. where NO+O$_2$ is the dominant channel and hot-band contributions are negligible (see below).

The RRKM rate for reaction (1) is given by:

$$k(E)=N^*(E-E_0)/hp(E), \qquad (3)$$

where $N^*(E-E_0)$ is the number of accessible transition state levels and $p(E)$ is the parent density of states. Use of the known NO$_3$ vibrational frequencies and the Whitten–Rabinovich approximation yields $p(E) \approx 100/$cm^{-1} for the ground ^{2}A$'_2$ surface at $E=16800$ cm^{-1}. By inserting $N^*(E-E_0)=1$ into eq. (3), and after multiplying by the degeneracy factor of 3 [32], the threshold rate is calculated to be 0.9×10^9 s^{-1}, in agreement with the experimental value of 1.0×10^9 s^{-1} at 16830 cm^{-1}. As shown in fig. 3a, the rise in $k(E)$ just above threshold can be simulated by using RRKM theory with a single transition state vibrational frequency near 70 cm^{-1}. The upward curvature in the plot of $k(E)$ vs. E near 17000 cm^{-1} suggests that a second low-frequency transition state vibrational mode contributes to the rate within 200 cm^{-1} of threshold. When using 70 and 140 cm^{-1} for the frequencies of the two accessible transition state modes, the RRKM rates were close to the experimental values (fig. 3). In principle, with sufficient resolution, good rotational cooling, and/or double resonance excitation, it might be possible to resolve step-like behavior in $k(E)$, as in previous experiments on NO$_2$ [3] and CH$_2$CO [8]. Due to the laser bandwidth of 60 cm^{-1} and relatively high rotational temperature (>30 K), this structure could not be resolved in the present experiment. Though our ad hoc estimates of NO$_3$ transition state vibrational frequencies led to RRKM rates in reasonable agreement with experiment, in the absence of further theoretical guidance we are reluctant to attribute quantitative significance to these parameters.

Molecules having two competing dissociation channels are particularly fascinating. In previous studies of photoinitiated NO$_3$ decomposition [19,22], it was concluded that the mechanism for NO production likely involves strong ^{2}E$'/^2$A$'_2$ coupling. The sharp decrease in NO signal above the NO$_2$+O threshold at 17040±90 cm^{-1} suggests competition between reactions (1) and (2). For competing decay channels from a common initial

ensemble of NO$_3$ levels, the measured rate for NO appearance is given (in the rate equation limit) by the sum of the rates for each channel. In this case, the NO signal is given by

$$S(t) \propto \frac{k_1}{k_1+k_2} \{1-\exp[-(k_1+k_2)t]\}. \qquad (4)$$

From eq. (4), the observation that the opening of the NO$_2$+O channel leads to a sharp decrease in the NO+O$_2$ signal amplitude near its threshold indicates that $k_2 \gg k_1$. We have not attempted a direct measurement of the rate of reaction (2) because of the large NO$_2$ background (which precludes the possibility of NO$_2$ detection by LIF or MPI) and the need for vacuum ultraviolet radiation for O atom detection. Though $k_2 \gg k_1$ is in accord with the sharp decrease in $S(t)$ above 17040 cm^{-1} [19], a quantitative determination of the NO$_2$+O decay rate, e.g. by measuring $S(t)$ above 17040 cm^{-1} and applying eq. (4), was not feasible. Above the NO$_2$+O threshold, the rate for simple O–NO$_2$ bond rupture increases much more rapidly than that for NO+O$_2$ production. Due to the substantial bandwidth of the pump laser used in the present experiments (≈ 60 cm^{-1}), the measured rate is an average over all of the prepared NO$_3$ levels in resonance with the laser source. As a result of this averaging, together with the sharp decrease in signal amplitude above D_0(O–NO$_2$), the sharp rise in the NO appearance rate could not be resolved. However, since the 0 K NO+O$_2$ quantum yield decreased from unity at 16970 cm^{-1} (where $k \approx 3 \times 10^9$ s^{-1}), to <1% at 17120 cm^{-1} [19], we infer from eq. (4) that $k_2 > 3 \times 10^{11}$ s^{-1} at 17120 cm^{-1}.

The sharply contrasting timescales for the two NO$_3$ dissociation channels provide insight into the mechanism for the NO$_2$+O channel. As shown in fig. 1, the NO+O$_2$ channel results from the decomposition highly vibrationally excited levels of the ground ^{2}A$'_2$ state, whereas both electronic states of NO$_3$ correlate with ground state NO$_2$+O. Nelson et al. estimated that the ^{2}A$'_2/^2$E$'$ coupling matrix element was small, on the order of 0.1 cm^{-1} [22]. Since O–NO$_2$ bond fission is closed below D_0(O–NO$_2$), the quantum yield for NO+O$_2$ will be unity despite the modest ^{2}A$'_2/^2$E$'$ coupling matrix element. However, above D_0(O–NO$_2$) the "bright" ^{2}E$'$ state couples much more strongly to the NO$_2$+O dissociation contin-

uum. The sparse $^2E'$ level density and small $^2A_2'/^2E'$ coupling matrix element leads to a small effective density of states. An excitation energy of 17120 cm^{-1} corresponds to 2070 cm^{-1} above the $^2E'$ origin. Although the vibrational frequencies of $NO_3(^2E')$ are not known, by using the ground state values we calculate $\rho(E) = 0.07/$cm^{-1} for $NO_3(^2E')$ at $E = 2070$ cm^{-1}. This corresponds to a threshold $NO_2 + O$ rate of 1.2×10^{12} s^{-1}, in accord with the inferred value of $> 3 \times 10^{11}$ s^{-1} presented above. We conclude that the Douglas effect, which plays an important part in the $NO + O_2$ channel, is not a significant factor in the production of $NO_2 + O$.

In a recent study of NO_3 photodissociation [19], hot bands were deemed responsible for a significant contribution from photodissociation of NO_3 molecules having at least one quantum of excitation in the doubly degenerate ν_4 mode (360 cm^{-1}). An important question is whether hot-band activity might play an important role in the rates observed in the present experiments. To assess this, we note that the NO quantum yield is known to be < 0.01 at excitation energies above 17100 cm^{-1} [19,23,24]. Assuming efficient rotational cooling in the supersonic expansion, absorption by $NO_3(0, 0, 0, 1)$ at photon energies above 16800 cm^{-1} must result in excitation to NO_3 levels lying above $D_0(O-NO_2)$, and these dissociate primarily to $NO_2 + O$ rather than $NO + O_2$ [19]. Consequently, hot-band activity cannot contribute significantly to the NO signal observed in the range 16800–17100 cm^{-1}, and these rates must arise from excitation of NO_3 in the ground vibrational state.

At photolysis energies below 16800 cm^{-1}, the NO signals were very weak. As shown in fig. 3, in this energy range, the reaction rate was found to *increase* substantially with decreasing energy. We attribute this to hot-band activity. The NO_3 decomposition rate resulting from absorption of a 16650 cm^{-1} photon was 4×10^9 s^{-1}. Interestingly, this lies close to the rate observed near 17000 cm^{-1}, i.e. ≈ 360 cm^{-1} higher. This suggests that the subnanosecond risetimes observed near 16650 cm^{-1} result primarily from excitation of $NO_3(0, 0, 0, 1)$ to levels lying approximately 17000 cm^{-1} above the ground state. From the temperature dependence of the absorption cross section, it is known that absorption in this wavelength region is not due exclusively to hot-bands

[32]. This is consistent with the earlier reports [20–22] that the NO_3 fluorescence intensity becomes substantial at excitation energies below 16800 cm^{-1}.

4. Conclusions

At energies just below $D_0(O-NO_2)$, the rates for photoinitiated unimolecular decomposition of NO_3 to $NO + O_2$ were found to be $(1-5) \times 10^9$ s^{-1}. By comparing the measured rates to those calculated by using RRKM theory, further evidence is provided that the reaction occurs on the ground $^2A_2'$ surface. From the measured $NO + O_2$ risetimes and previously measured quantum yields, we infer that the rate for simple $O-NO_2$ fission exceeds 3×10^{11} at 17050 cm^{-1}. This is in accord with RRKM estimates, assuming that simple $O-NO_2$ bond fission occurs on the excited $^2E'$ surface.

References

[1] H. Reisler and C. Wittig, Ann. Rev. Phys. Chem. 37 (1986) 307, and references therein.
[2] M.N.R. Ashfold and J.E. Baggott, eds. Molecular photodissociation dynamics (Roy. Soc. Chem., Bridgeport, 1989), and references therein.
[3] G.A. Brucker, S.I. Ionov, Y. Chen and C. Wittig, Chem. Phys. Letters 194 (1992) 301.
[4] S.I. Ionov, G.A. Brucker, C. Jaques, Y. Chen and C. Wittig, J. Chem. Phys. 99 (1993) 3420.
[5] C.B. Moore and J.C. Weisshaar, Ann. Rev. Phys. Chem. 34 (1983) 525, and references therein.
[6] W.H. Green Jr., C.B. Moore and W.F. Polik, Ann. Rev. Phys. Chem. 43 (1992) 591.
[7] R.D. van Zee, C.D. Pibel, T.J. Butenhoff and C.B. Moore, J. Chem. Phys. 97 (1992) 3235.
[8] E.R. Lovejoy, S.K. Kim and C.B. Moore, Science 256 (1992) 1541.
[9] L.R. Khundkar and A.H. Zewail, Ann. Rev. Phys. Chem. 41 (1990) 15.

[10] A.H. Zewail, Faraday Discussions Chem. Soc. 91 (1991) 207.

[11] S.J. Klippenstein and T. Radivoyevitch, J. Chem. Phys. 99 (1993) 3644.

[12] E.F. Cromwell, A. Stolow, M.J.J. Vrakking and Y.T. Lee, J. Chem. Phys. 97 (1992) 4029.

[13] Aa.S. Sudbo, P.A. Schulz, Y.R. Shen and Y.T. Lee, J. Chem. Phys. 69 (1978) 2312.

[14] D. Krajnovich, F. Huisken, Z. Zhang, Y.R. Shen and Y.T. Lee, J. Chem. Phys. 77 (1982) 5977.

[15] J.W. Hudgens, J. Chem. Phys. 68 (1978) 777.

[16] R.P. Wayne, I. Barnes, P. Biggs, J.P. Burrows, C.E. Canosa-Mas, J. Hjorth, G. LeBras, G.K. Moortgat, D. Perner, G. Poulet, G. Restelli and H. Sidebottom, in : The nitrate radical: physics, chemistry, and the atmosphere (1990). Air Pollution Research Report 31 (1990).

[17] J.P. Smith and S. Solomon, J. Geophys. Res. 95 D9 (1990) 13, 819.

[18] G.A. Olah and D.R. Squire, eds., Chemistry of energetic materials (Academic Press, New York, 1991).

[19] H.F. Davis, B. Kim, H.S. Johnston and Y.T. Lee, J. Phys. Chem. 97 (1993) 2172.

[20] H.H. Nelson, L. Pasternack and J.R. McDonald, J. Phys. Chem. 87 (1983) 1286.

[21] T. Ishiwata, I. Fujiwara, Y. Naruge, K. Obi and I. Tanaka, J. Phys. Chem. 87 (1983) 1349.

[22] H.H. Nelson, L. Pasternack and J.R. McDonald, J. Chem. Phys. 79 (1983) 4279.

[23] F. Magnotta and H.S. Johnston, Geophys. Res. Letters 7 (1980) 769.

[24] F. Magnotta, Ph.D. Thesis, University of California, Berkeley (1979), Lawrence Berkeley Laboratory Report LBL-9981.

[25] R.A. Graham and H.S. Johnston, J. Phys. Chem. 82 (1978) 254.

[26] E. Hirota, K. Kawaguchi, T. Ishiwata and I. Tanaka, J. Chem. Phys. 95 (1991) 771.

[27] A.E. Douglas, J. Chem. Phys. 45 (1966) 1007.

[28] S.I. Ionov, G.A. Brucker, C. Jaques, L. Valachovic and C. Wittig, J. Chem. Phys. 97 (1992) 9486.

[29] H.S. Johnston, Gas phase reaction rate theory (Ronald, New York, 1966).

[30] B. Kim, Ph.D. Thesis, University of California, Berkeley, (1990); Lawrence Berkeley Laboratory Report LBL-29688.

[31] H.S. Johnston and R.A. Graham, Can. J. Chem. 52 (1974) 1415.

[32] S.P. Sander, J. Phys. Chem. 90 (1986) 4135, and references therein.

[33] P.J. Robinson and K.A. Holbrook, Unimolecular reactions (Wiley, New York, 1972).

[34] P.E.M. Siegbahn, J. Comput. Chem. 6 (1985) 182.

[35] R.C. Boehm, Ph.D. Thesis, University of Michigan (1990).

[36] R.C. Boehm, private communication.

[37] J.F. Stanton, J. Gauss and R.J. Bartlett, J. Chem. Phys. 94 (1991) 4084.

[38] R.D. Davy and H.F. Schaefer III, J. Chem. Phys. 91 (1989) 4410.